Lanthanide-EDTA complexes covalently bonded on Fe₃O₄@SiO₂ magnetic nanoparticles promote the green, stereoselective synthesis of *N*-acylhydrazones

João Batista M. de Resende Filho[1], Nathália Kellyne S. M. Falcão[2], Gilvan P. Pires[2], Luiz Fernando S. de Vasconcelos[2], Sávio M. Pinheiro[2], José Maurício dos Santos Filho[3], Marília Imaculada Frazão Barbosa[4], Antônio Carlos Doriguetto[4], Ercules E. S. Teotonio[2], Juliana A. Vale[2],*

[1]Instituto Federal de Educação, Ciência e Tecnologia da Paraíba, Campus Sousa. Av. Presidente Tancredo Neves, s/n – Jardim Sorrilândia, 58800-970, Sousa (PB), Brazil. Phone: +55-83-3522-2727.

[2]Departamento de Química, Universidade Federal da Paraíba, 58051-970 João Pessoa-PB, Brazil. Phone: +55-83-3216-7591. Fax: +55-83-3216-7437.

[3]Laboratório de Planejamento e Síntese Aplicados à Química Medicinal – *SintMed*®, Universidade Federal de Pernambuco, 50740-521, Recife, PE, Brazil. Phone: +55-81-2126-3008

[4]Instituto de Química, Universidade Federal de Alfenas, CEP 37130-000, Alfenas-MG, Brazil.

*Corresponding author. E-mail: julianadqf@yahoo.com.br

SPECTRA FOR DATA CONFIRMATION

**Figure S1.** ¹H NMR spectrum of compound (**1**), *N'*-(4-hydroxy-3-methoxybenzylidene)benzohydrazide.
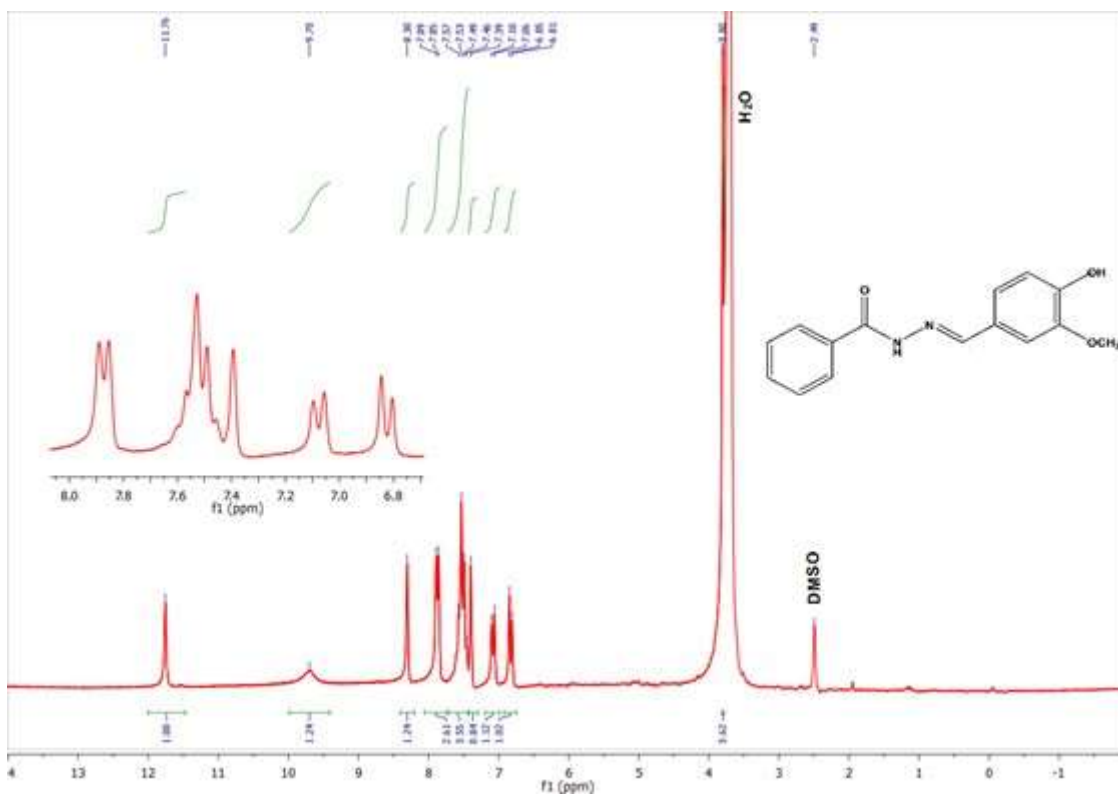
**Figure S2.** ¹H NMR spectrum of compound **(2)**, *N'*-benzylidenebenzohydrazide.
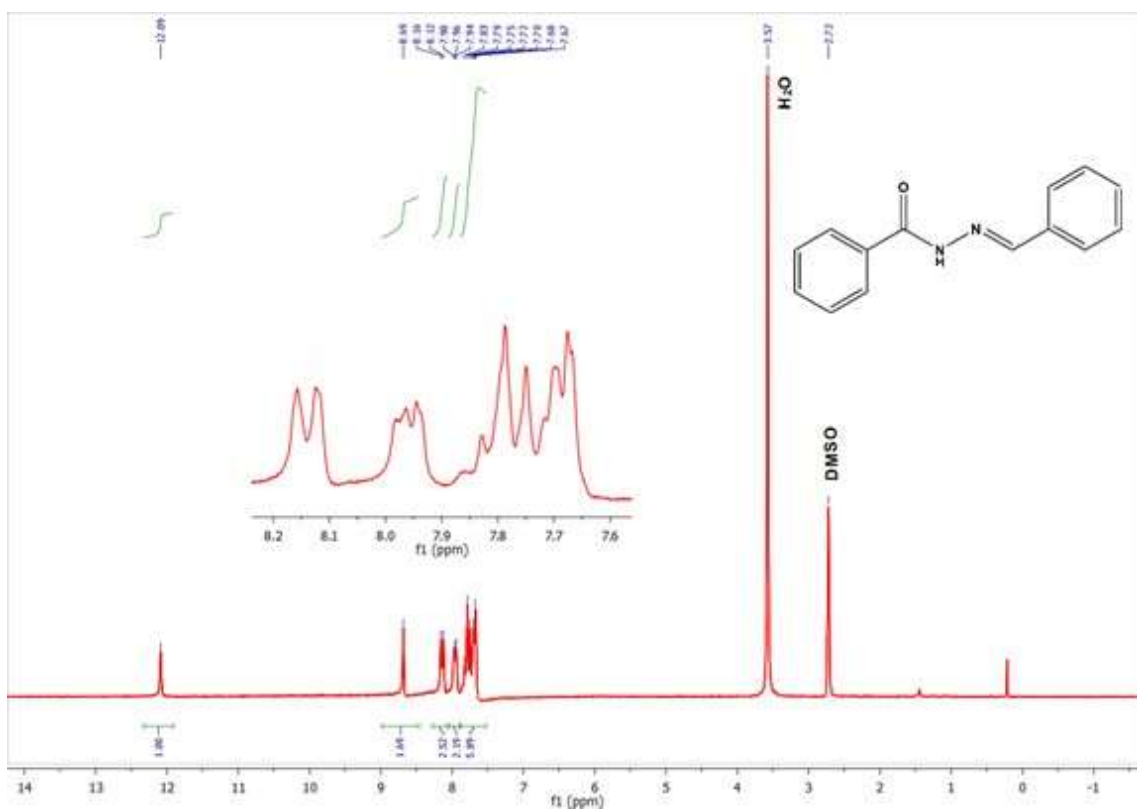
**Figure S3.** ¹H NMR spectrum of compound **(3)**, *N'*-benzylidene-4-methoxybenzohydrazide.
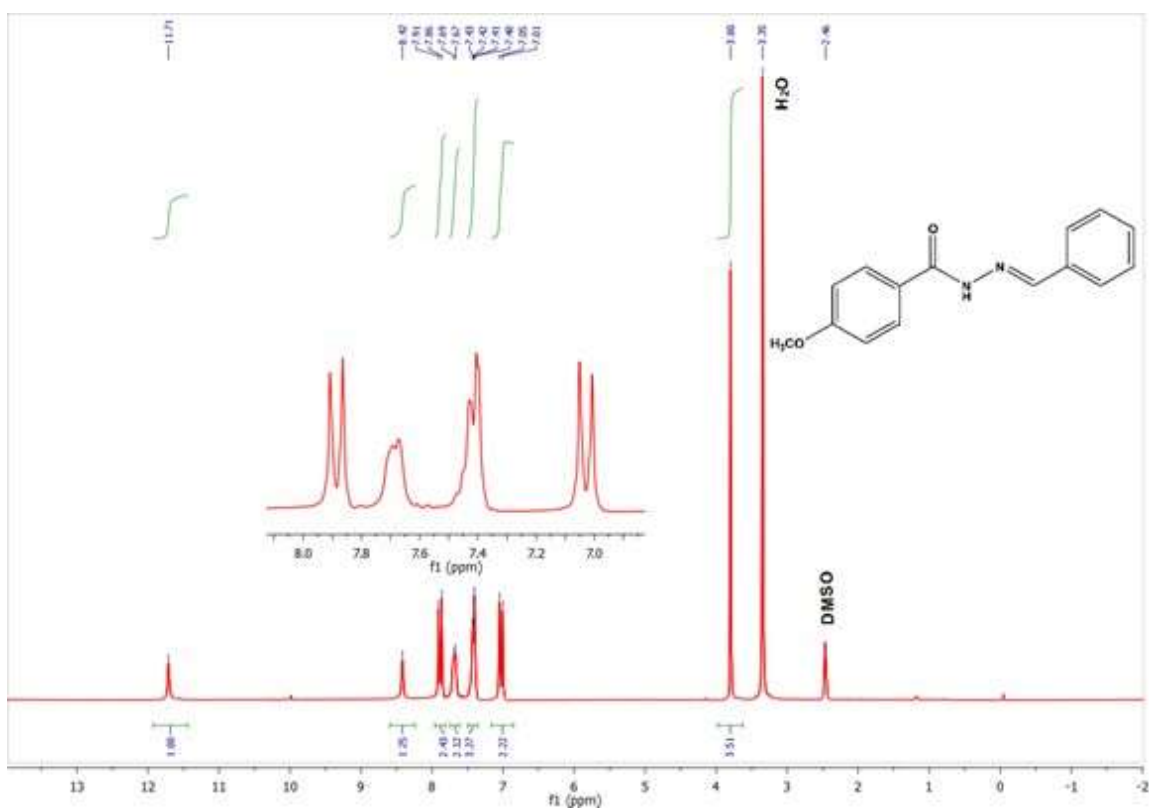
Figure S4. ^{1}H NMR spectrum of compound **(4)**, *N'*-benzylidene-3,5-dinitroxybenzohydrazide.
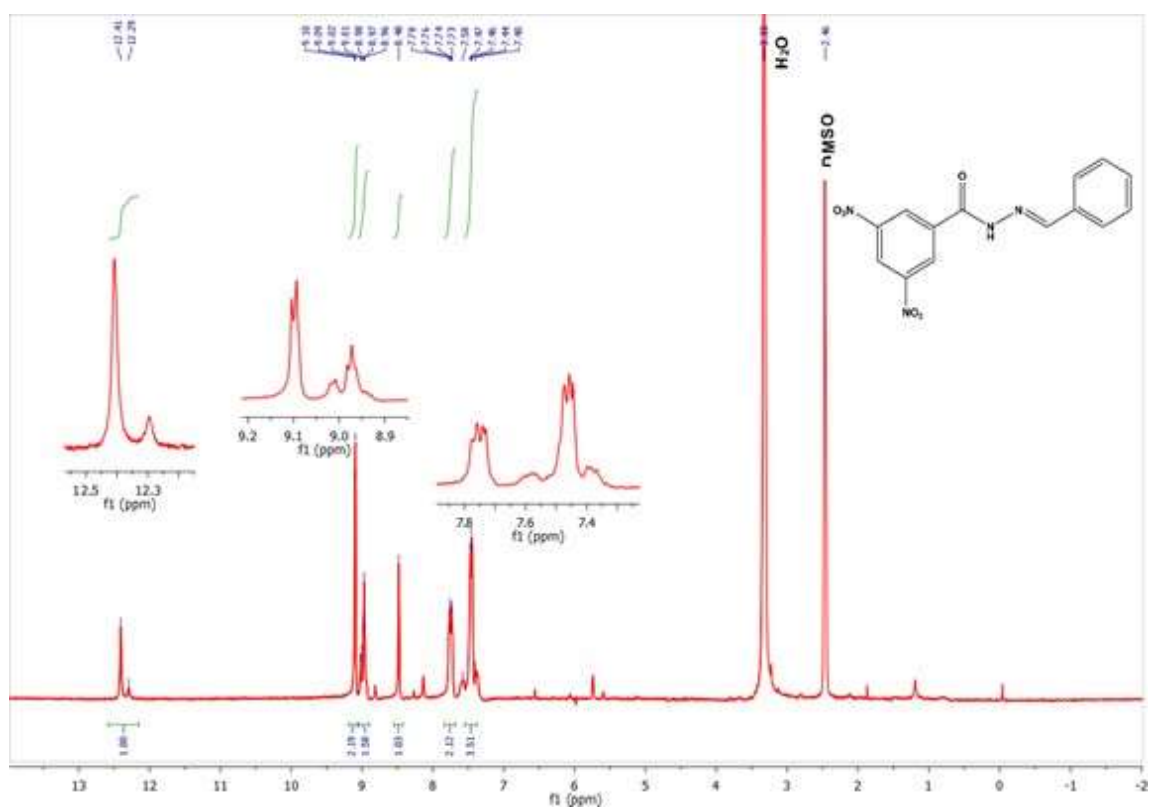

Figure S5. ^{1}H NMR spectrum of compound **(5)**, *N'*-benzylidene-4-nitrobenzohydrazide.
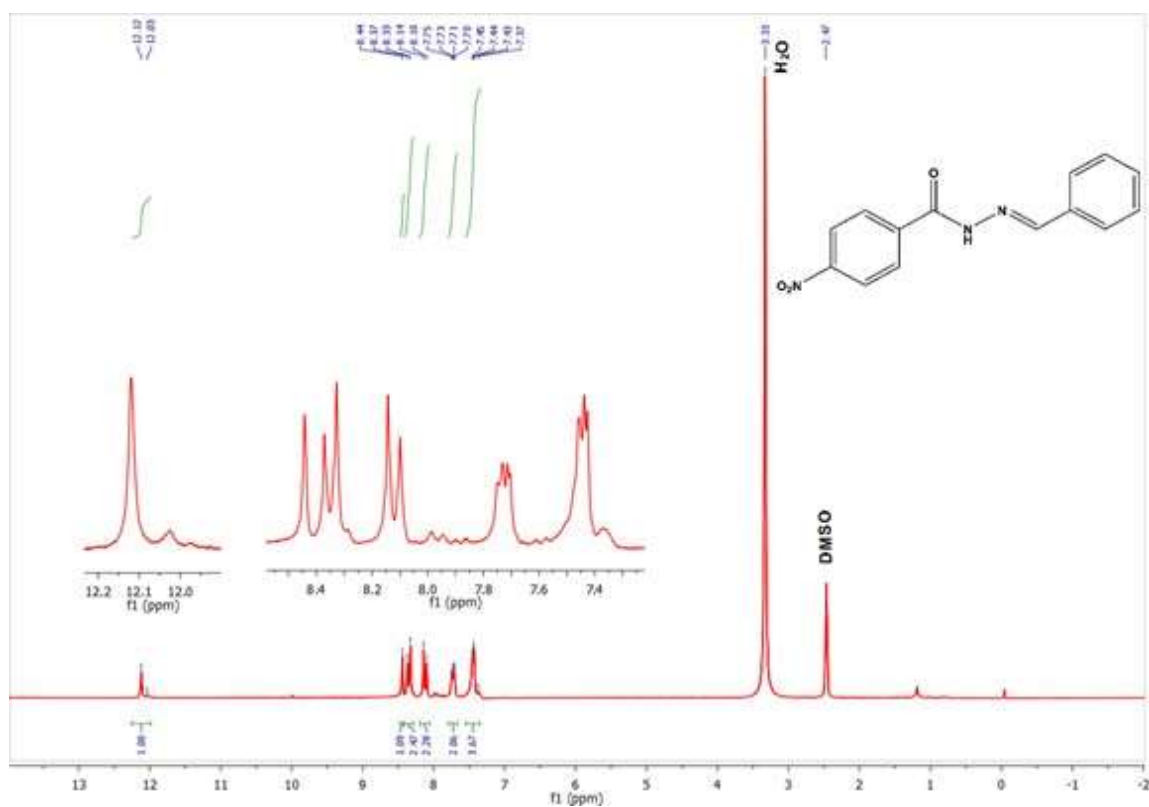
Figure S6. ^{1}H NMR spectrum of compound **(6)**, *N'*-(2-nitrobenzylidene)benzohydrazide.
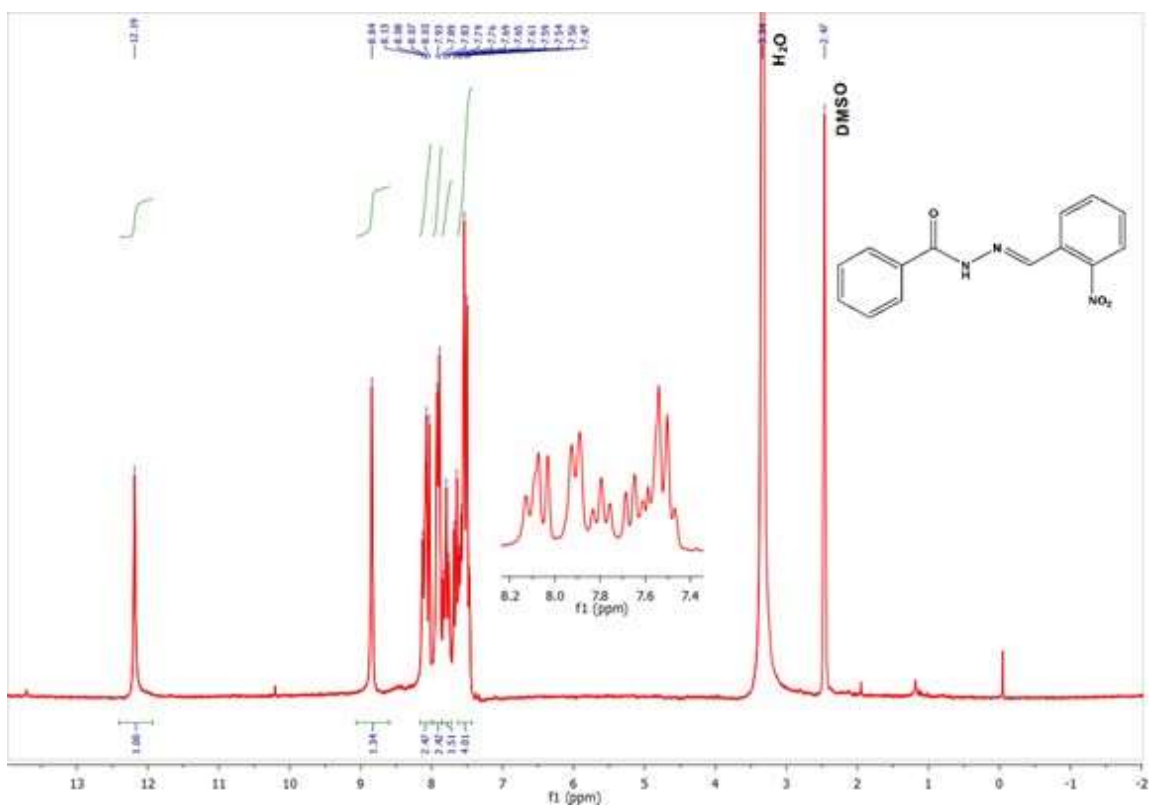
Figure S7. ^{1}H NMR spectrum of compound **(7)**, *N'*-(4-nitrobenzylidene)benzohydrazide.
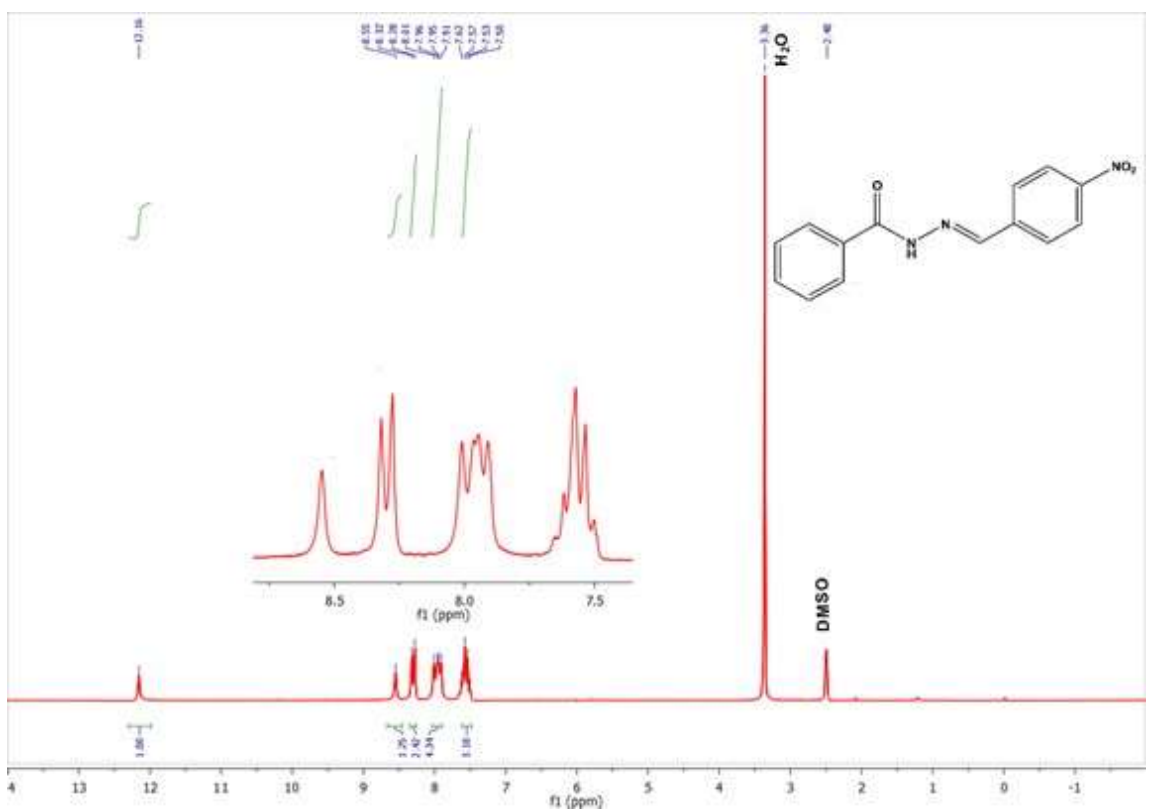
Figure S8. ^{1}H NMR spectrum of compound **(8)**, *N'*-(4-methoxybenzylidene)benzohydrazide.
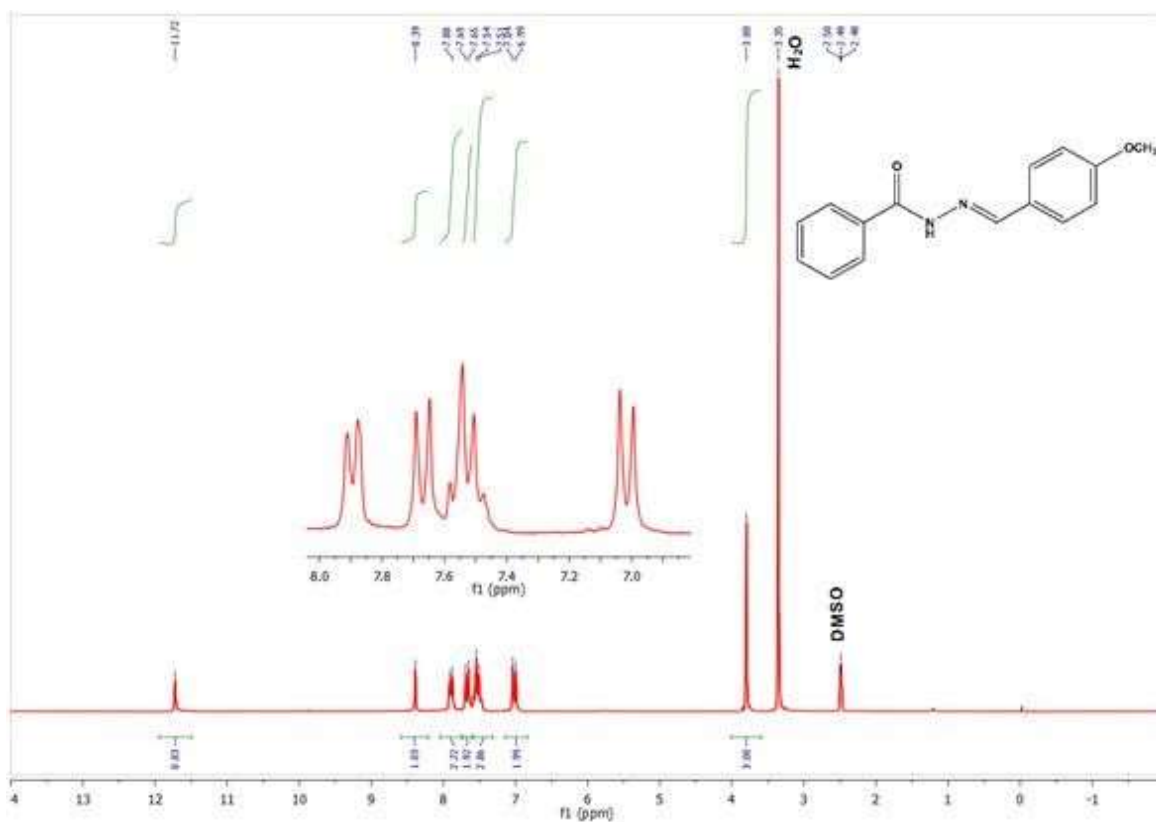
Figure S9. ^{1}H NMR spectrum of compound **(9)**, *N'*-cyclohexylidenebenzohydrazide.
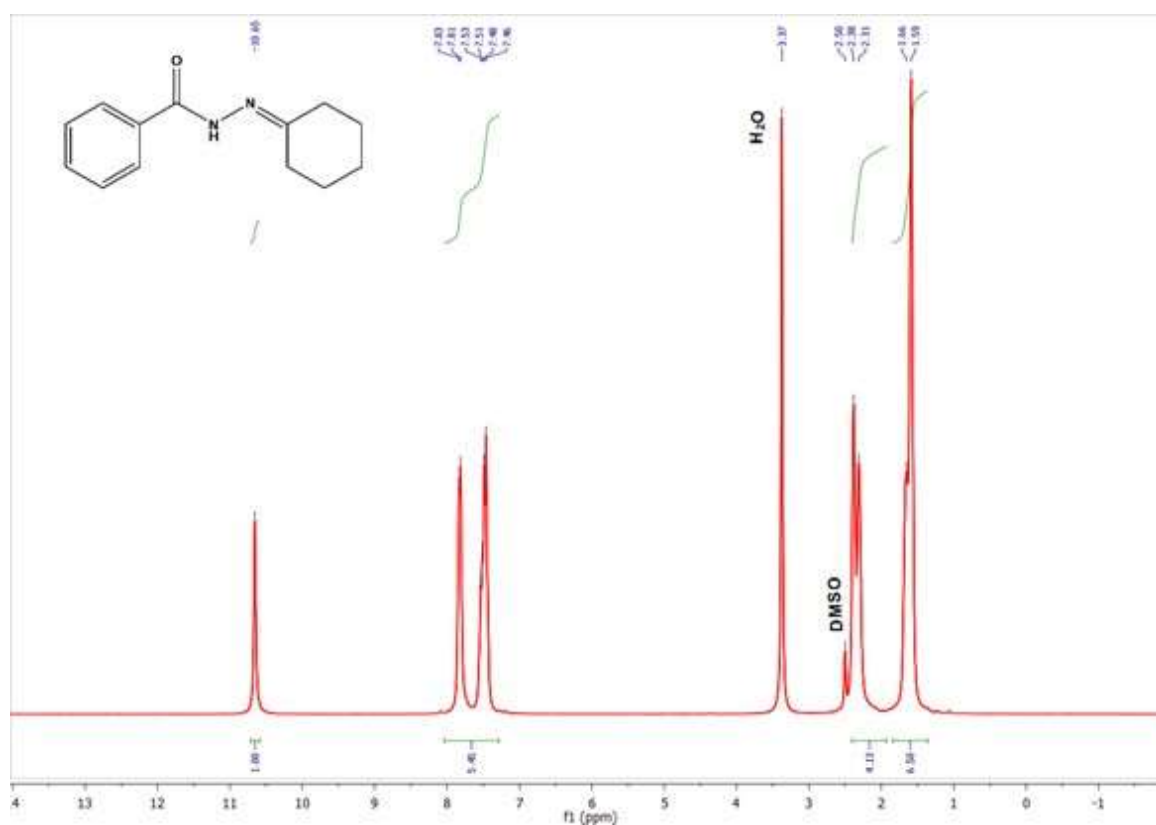
Figure S10. ^{1}H NMR spectrum of compound **(10)**, *N'*-(butan-2-ylidene)benzohydrazide.
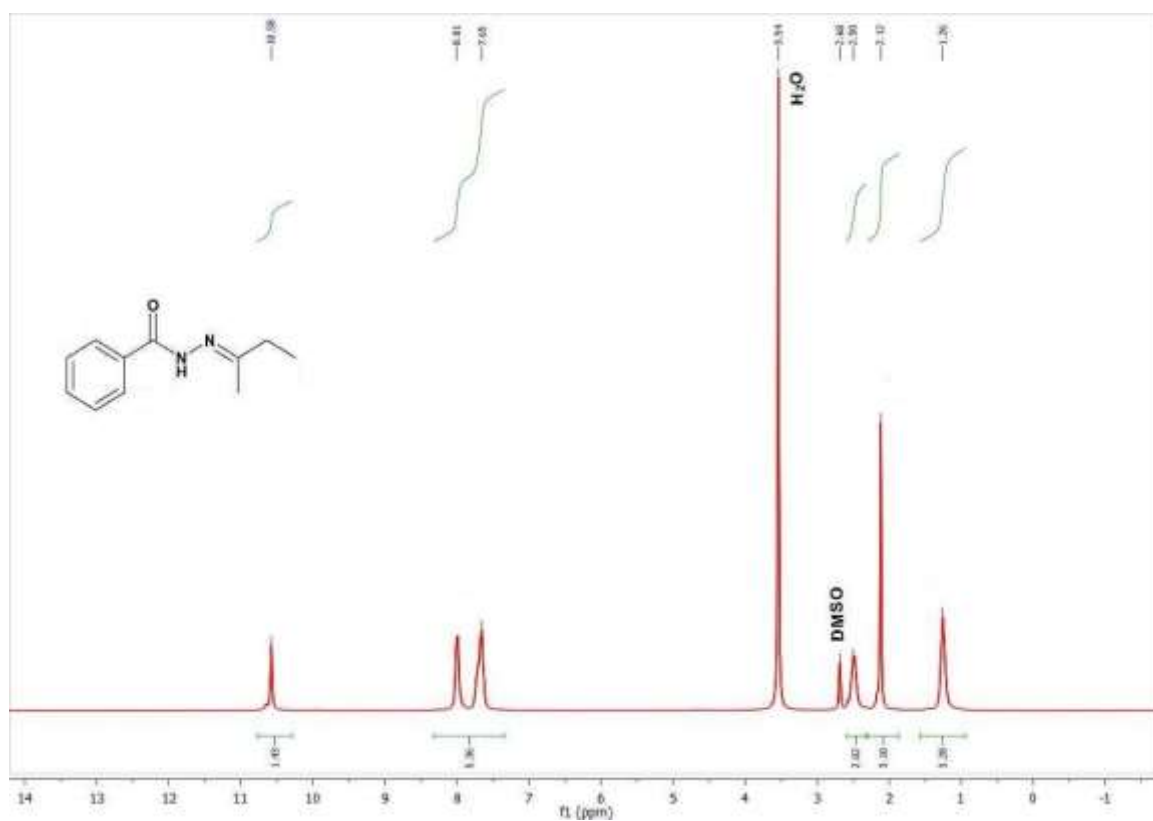
Figure S11. ^{1}H NMR spectrum of compound **(11)**, *N'*-(1-phenylethylidene)benzohydrazide.
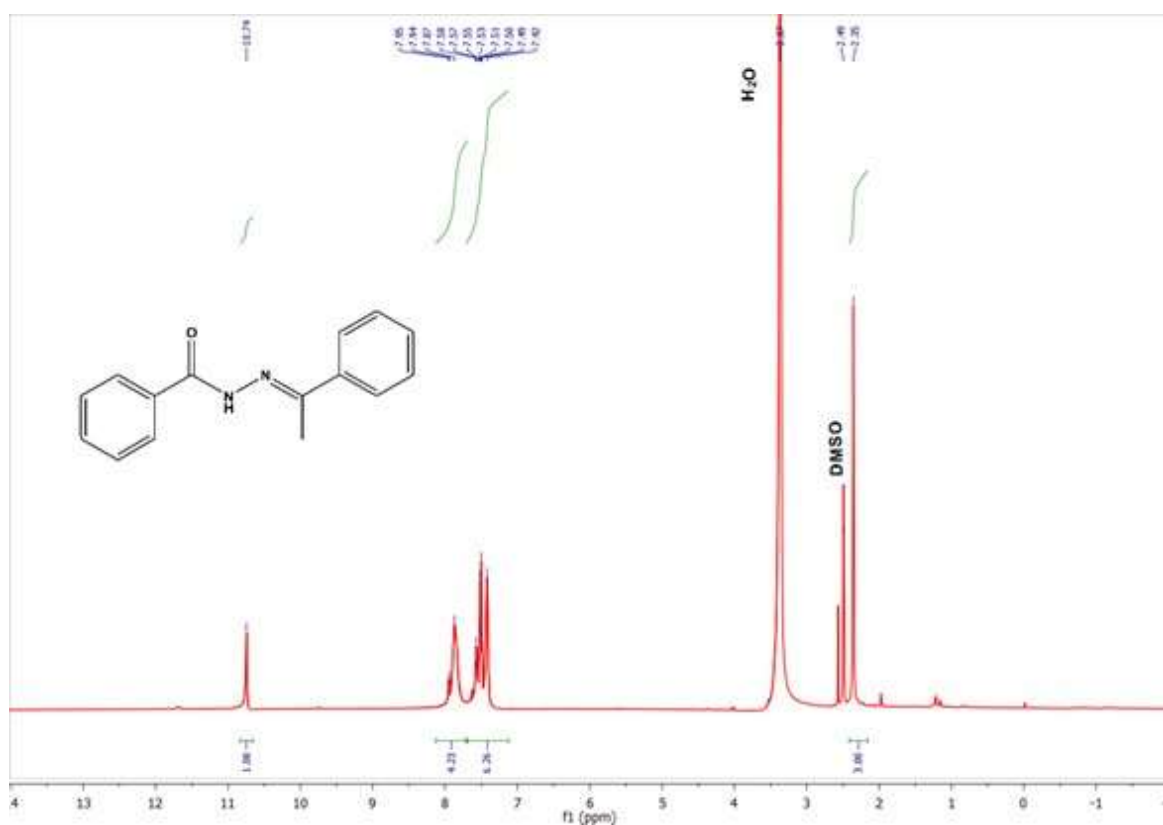
Figure S12. ^{1}H NMR spectrum of compound **(12)**, *N'*-cyclohexylidene-4-aminebenzohydrazide.
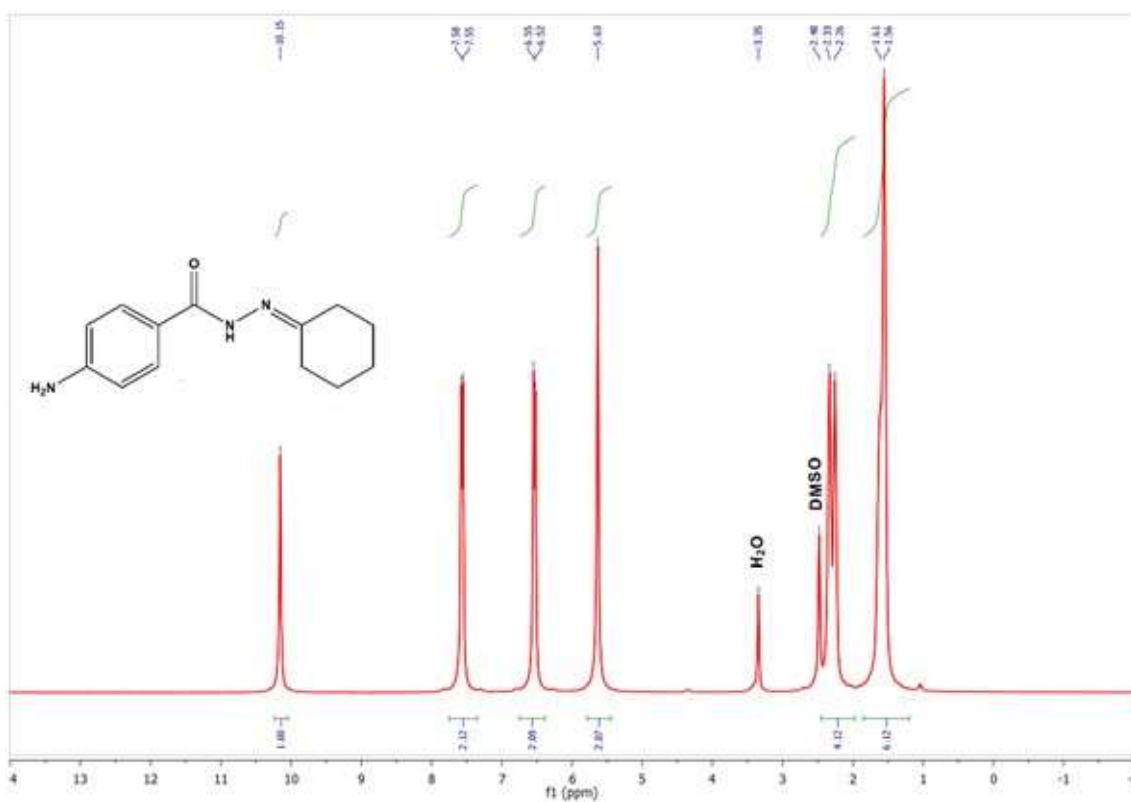
**Figure S13.** ^{1}H NMR spectrum of compound **(13)**, *N'*-cyclohexylidene-4-nitrobenzohydrazide.
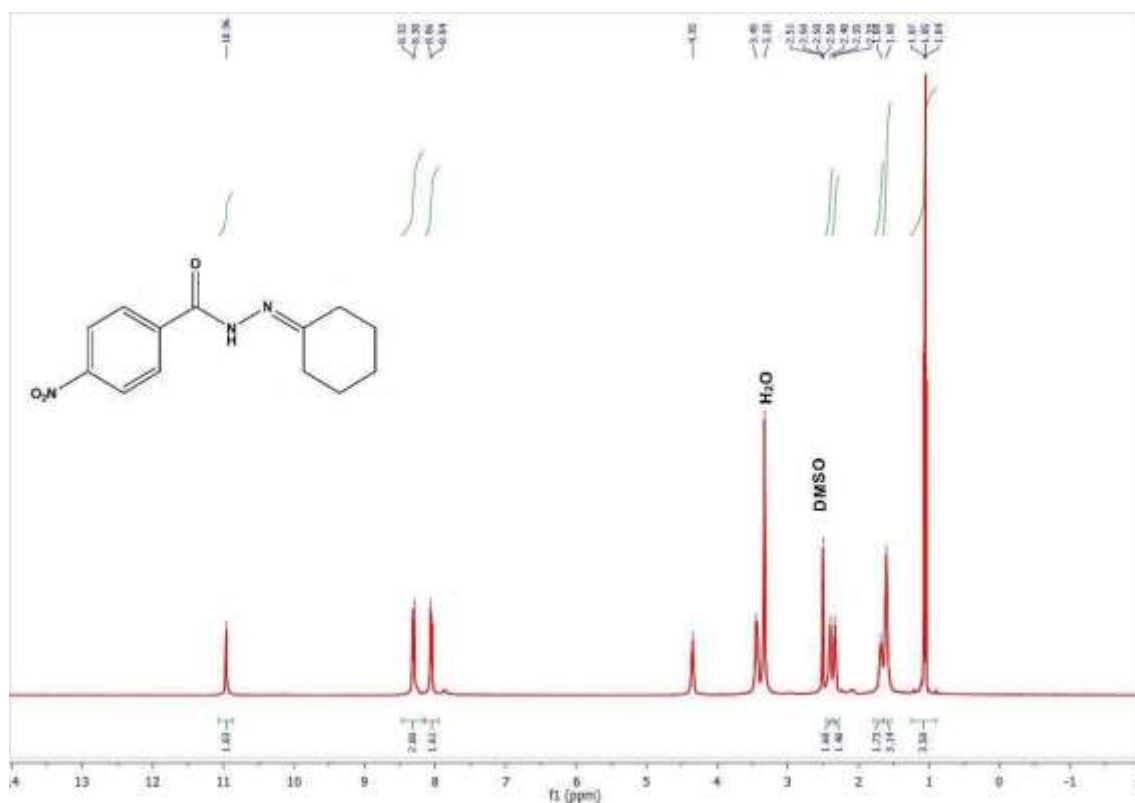
Figure S14. ^{1}H NMR spectrum of compound **(14)**, 3-(4-tolyl)-*N'*-(*E*-ferrocenylmethylidene)-1,2,4-oxadiazol-5-ylcarbohydrazide.
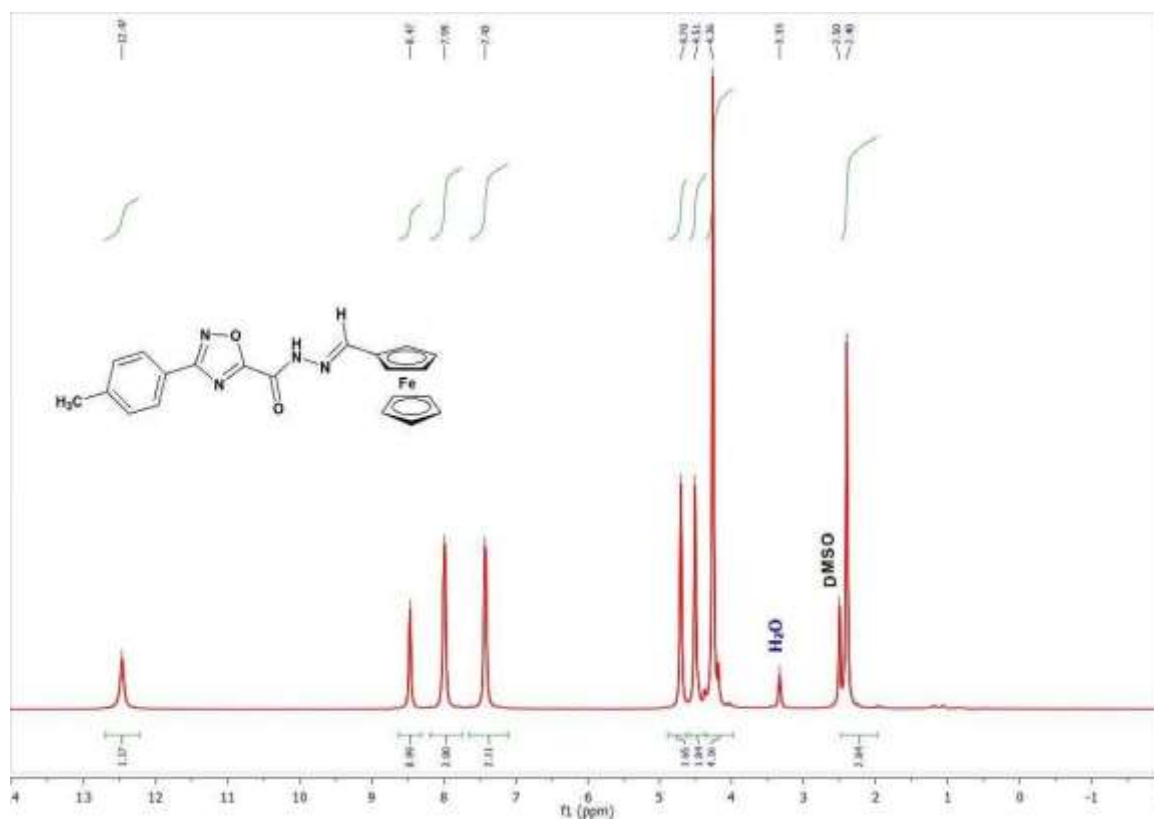
CRYSTALLOGRAPHIC DATA FOR 3-(4-TOLYL)-*N'*-(*E*-FERROCENYLMETHYLIDENE)-1,2,4-OXADIAZOL-5-YLCARBOHYDRAZIDE-COMPOUND 14

The following crystal has been deposited at the Cambridge Crystallographic Data Center and allocated the deposition number CCDC 1859291.

Table 1. Crystal data and structure refinement for **14**.

Identification code	shelxl
Empirical formula	C17 H13 Fe N O
Formula weight	303.13
Temperature	296(2) K
Wavelength	0.71073 Å
Crystal system	Orthorhombic
Space group	P c a 21
Unit cell dimensions	a = 19.016(16) Å $\alpha = 90°$.
	b = 12.875(8) Å $\beta = 90°$.
	c = 7.696(5) Å $\gamma = 90°$.
Volume	1884(2) $Å^3$
Z	4
Density (calculated)	1.069 Mg/m^3
Absorption coefficient	0.795 mm^{-1}
F(000)	624
Theta range for data collection	1.582 to 25.369°.
Index ranges	-22<=h<=5, -15<=k<=9, -7<=l<=7
Reflections collected	4325
Independent reflections	2490 [R(int) = 0.0494]
Completeness to theta = 25.242°	81.3 %
Refinement method	Full-matrix least-squares on F^2
Data / restraints / parameters	2490 / 169 / 253
Goodness-of-fit on F^2	1.011
Final R indices [I>2sigma(I)]	R1 = 0.0645, wR2 = 0.1562
R indices (all data)	R1 = 0.1099, wR2 = 0.2004
Absolute structure parameter	0.31(4)
Extinction coefficient	n/a
Largest diff. peak and hole	0.312 and -0.299 $e.Å^{-3}$

Table 2. Atomic coordinates (x 10^4) and equivalent isotropic displacement parameters (Å^2x 10^3) for m71. U(eq) is defined as one third of the trace of the orthogonalized U^{ij} tensor.

	x	y	z	U(eq)
Fe(1)	6116(1)	-1723(1)	7603(3)	55(1)
C(2)	8737(8)	4846(11)	16690(30)	67(5)
C(14)	5730(9)	-1351(13)	5160(20)	72(5)
C(15)	5209(7)	-1301(12)	6440(20)	68(4)
C(16)	5429(6)	-568(10)	7720(30)	64(4)
C(12)	6082(7)	-162(11)	7170(20)	65(6)
C(11)	6516(7)	495(11)	8213(18)	58(4)
N(4)	7117(5)	799(7)	7758(18)	52(3)
N(3)	7494(6)	1394(7)	8900(17)	53(3)
C(9)	8479(7)	2319(13)	9900(20)	63(4)
C(8)	8809(6)	3137(11)	12020(17)	43(4)
N(2)	8240(5)	2843(9)	11114(18)	53(3)
C(5)	8789(7)	3714(10)	13660(20)	51(4)
C(4)	9388(7)	3852(13)	14640(20)	67(5)
C(6)	8169(7)	4108(11)	14220(20)	59(4)
O(1)	9172(6)	2206(11)	9872(15)	92(4)
C(7)	8131(8)	4697(12)	15720(20)	67(4)
C(10)	8131(7)	1775(11)	8480(20)	58(4)
N(1)	9427(8)	2734(14)	11380(20)	102(5)
O(2)	8378(5)	1674(8)	7036(15)	77(4)
C(13)	6286(7)	-681(11)	5670(20)	60(4)
C(3)	9339(8)	4408(14)	16170(20)	81(5)
C(1)	8721(9)	5437(15)	18320(20)	96(7)
C(19)	6310(20)	-3247(19)	7870(40)	136(11)
C(20)	5949(13)	-2980(20)	9100(40)	118(9)
C(18)	6908(14)	-2710(30)	7910(60)	170(18)
C(22)	6290(30)	-2250(30)	10070(40)	166(16)
C(17)	6880(20)	-2030(30)	9200(70)	190(20)

Table 3. Bond lengths [Å] and angles [°] for **14**.

Fe(1)-C(17)	1.95(2)
Fe(1)-C(16)	1.982(12)
Fe(1)-C(18)	1.98(2)
Fe(1)-C(20)	2.01(2)
Fe(1)-C(15)	2.017(14)
Fe(1)-C(19)	2.01(2)
Fe(1)-C(13)	2.031(15)
Fe(1)-C(12)	2.038(14)
Fe(1)-C(14)	2.072(17)
Fe(1)-C(22)	2.05(3)
C(2)-C(3)	1.338(19)
C(2)-C(7)	1.39(2)
C(2)-C(1)	1.46(2)
C(14)-C(15)	1.40(2)
C(14)-C(13)	1.42(2)
C(14)-H(14)	0.9300
C(15)-C(16)	1.43(2)
C(15)-H(15)	0.9300
C(16)-C(12)	1.411(18)
C(16)-H(16)	0.9300
C(12)-C(13)	1.39(2)
C(12)-C(11)	1.428(19)
C(11)-N(4)	1.257(16)
C(11)-H(11)	0.9300
N(4)-N(3)	1.368(15)
N(3)-C(10)	1.347(18)
N(3)-H(3N)	0.8600
C(9)-N(2)	1.24(2)
C(9)-O(1)	1.326(16)
C(9)-C(10)	1.46(2)
C(9)-C(8)	2.04(2)
C(8)-N(2)	1.342(17)
C(8)-N(1)	1.376(17)
C(8)-C(5)	1.46(2)
C(5)-C(6)	1.356(18)
C(5)-C(4)	1.38(2)

C(4)-C(3)	1.38(2)
C(4)-H(4)	0.9300
C(6)-C(7)	1.38(2)
C(6)-H(6)	0.9300
O(1)-N(1)	1.428(17)
C(7)-H(7)	0.9300
C(10)-O(2)	1.211(17)
C(13)-H(13)	0.9300
C(3)-H(3)	0.9300
C(1)-H(1A)	0.9600
C(1)-H(1B)	0.9600
C(1)-H(1C)	0.9600
C(19)-C(20)	1.22(4)
C(19)-C(18)	1.33(4)
C(19)-H(19)	0.9300
C(20)-C(22)	1.36(4)
C(20)-H(20)	0.9300
C(18)-C(17)	1.32(5)
C(18)-H(18)	0.9300
C(22)-C(17)	1.34(5)
C(22)-H(21)	0.9300
C(17)-H(17)	0.9300
C(17)-Fe(1)-C(16)	128.2(18)
C(17)-Fe(1)-C(18)	39.2(15)
C(16)-Fe(1)-C(18)	167.2(16)
C(17)-Fe(1)-C(20)	66.0(12)
C(16)-Fe(1)-C(20)	118.4(9)
C(18)-Fe(1)-C(20)	62.4(10)
C(17)-Fe(1)-C(15)	167(2)
C(16)-Fe(1)-C(15)	41.7(7)
C(18)-Fe(1)-C(15)	151.0(15)
C(20)-Fe(1)-C(15)	109.7(9)
C(17)-Fe(1)-C(19)	66.3(13)
C(16)-Fe(1)-C(19)	148.3(12)
C(18)-Fe(1)-C(19)	39.0(11)
C(20)-Fe(1)-C(19)	35.3(11)
C(15)-Fe(1)-C(19)	117.8(11)

C(17)-Fe(1)-C(13)	118.5(11)
C(16)-Fe(1)-C(13)	69.0(6)
C(18)-Fe(1)-C(13)	112.9(10)
C(20)-Fe(1)-C(13)	167.5(12)
C(15)-Fe(1)-C(13)	68.4(6)
C(19)-Fe(1)-C(13)	133.7(12)
C(17)-Fe(1)-C(12)	109.0(10)
C(16)-Fe(1)-C(12)	41.1(5)
C(18)-Fe(1)-C(12)	132.3(12)
C(20)-Fe(1)-C(12)	151.9(11)
C(15)-Fe(1)-C(12)	68.6(6)
C(19)-Fe(1)-C(12)	170.5(13)
C(13)-Fe(1)-C(12)	40.0(6)
C(17)-Fe(1)-C(14)	152.0(18)
C(16)-Fe(1)-C(14)	68.5(8)
C(18)-Fe(1)-C(14)	121.7(14)
C(20)-Fe(1)-C(14)	130.5(12)
C(15)-Fe(1)-C(14)	39.9(7)
C(19)-Fe(1)-C(14)	112.6(10)
C(13)-Fe(1)-C(14)	40.4(6)
C(12)-Fe(1)-C(14)	67.3(7)
C(17)-Fe(1)-C(22)	39.2(14)
C(16)-Fe(1)-C(22)	108.6(11)
C(18)-Fe(1)-C(22)	63.3(14)
C(20)-Fe(1)-C(22)	39.2(12)
C(15)-Fe(1)-C(22)	129.9(14)
C(19)-Fe(1)-C(22)	63.1(11)
C(13)-Fe(1)-C(22)	151.2(14)
C(12)-Fe(1)-C(22)	119.1(10)
C(14)-Fe(1)-C(22)	167.5(15)
C(3)-C(2)-C(7)	119.2(18)
C(3)-C(2)-C(1)	119.7(16)
C(7)-C(2)-C(1)	121.0(16)
C(15)-C(14)-C(13)	108.0(15)
C(15)-C(14)-Fe(1)	67.9(10)
C(13)-C(14)-Fe(1)	68.3(9)
C(15)-C(14)-H(14)	126.0
C(13)-C(14)-H(14)	126.0

Fe(1)-C(14)-H(14)	129.4
C(14)-C(15)-C(16)	107.9(14)
C(14)-C(15)-Fe(1)	72.2(10)
C(16)-C(15)-Fe(1)	67.8(8)
C(14)-C(15)-H(15)	126.0
C(16)-C(15)-H(15)	126.0
Fe(1)-C(15)-H(15)	125.6
C(12)-C(16)-C(15)	107.4(16)
C(12)-C(16)-Fe(1)	71.6(7)
C(15)-C(16)-Fe(1)	70.5(8)
C(12)-C(16)-H(16)	126.3
C(15)-C(16)-H(16)	126.3
Fe(1)-C(16)-H(16)	123.3
C(13)-C(12)-C(16)	108.3(14)
C(13)-C(12)-C(11)	126.1(13)
C(16)-C(12)-C(11)	124.2(17)
C(13)-C(12)-Fe(1)	69.7(8)
C(16)-C(12)-Fe(1)	67.3(8)
C(11)-C(12)-Fe(1)	118.4(11)
N(4)-C(11)-C(12)	123.6(13)
N(4)-C(11)-H(11)	118.2
C(12)-C(11)-H(11)	118.2
C(11)-N(4)-N(3)	118.1(12)
C(10)-N(3)-N(4)	121.3(13)
C(10)-N(3)-H(3N)	119.4
N(4)-N(3)-H(3N)	119.4
N(2)-C(9)-O(1)	115.8(14)
N(2)-C(9)-C(10)	131.4(13)
O(1)-C(9)-C(10)	112.7(15)
N(2)-C(9)-C(8)	39.5(8)
O(1)-C(9)-C(8)	76.3(9)
C(10)-C(9)-C(8)	171.0(12)
N(2)-C(8)-N(1)	113.3(13)
N(2)-C(8)-C(5)	124.7(11)
N(1)-C(8)-C(5)	121.6(12)
N(2)-C(8)-C(9)	36.0(7)
N(1)-C(8)-C(9)	77.3(10)
C(5)-C(8)-C(9)	160.4(10)

C(9)-N(2)-C(8)	104.4(11)
C(6)-C(5)-C(4)	119.6(16)
C(6)-C(5)-C(8)	119.3(13)
C(4)-C(5)-C(8)	121.0(13)
C(3)-C(4)-C(5)	118.5(14)
C(3)-C(4)-H(4)	120.7
C(5)-C(4)-H(4)	120.7
C(5)-C(6)-C(7)	121.2(14)
C(5)-C(6)-H(6)	119.4
C(7)-C(6)-H(6)	119.4
C(9)-O(1)-N(1)	105.8(12)
C(2)-C(7)-C(6)	118.9(15)
C(2)-C(7)-H(7)	120.5
C(6)-C(7)-H(7)	120.5
O(2)-C(10)-N(3)	122.1(16)
O(2)-C(10)-C(9)	124.2(14)
N(3)-C(10)-C(9)	113.6(14)
C(8)-N(1)-O(1)	100.4(12)
C(12)-C(13)-C(14)	108.2(13)
C(12)-C(13)-Fe(1)	70.2(9)
C(14)-C(13)-Fe(1)	71.3(9)
C(12)-C(13)-H(13)	125.9
C(14)-C(13)-H(13)	125.9
Fe(1)-C(13)-H(13)	124.1
C(2)-C(3)-C(4)	122.3(15)
C(2)-C(3)-H(3)	118.8
C(4)-C(3)-H(3)	118.8
C(2)-C(1)-H(1A)	109.5
C(2)-C(1)-H(1B)	109.5
H(1A)-C(1)-H(1B)	109.5
C(2)-C(1)-H(1C)	109.5
H(1A)-C(1)-H(1C)	109.5
H(1B)-C(1)-H(1C)	109.5
C(20)-C(19)-C(18)	108(3)
C(20)-C(19)-Fe(1)	72.6(14)
C(18)-C(19)-Fe(1)	69.4(16)
C(20)-C(19)-H(19)	125.8
C(18)-C(19)-H(19)	125.8

Fe(1)-C(19)-H(19)	123.8
C(19)-C(20)-C(22)	110(3)
C(19)-C(20)-Fe(1)	72.1(16)
C(22)-C(20)-Fe(1)	71.7(16)
C(19)-C(20)-H(20)	124.8
C(22)-C(20)-H(20)	124.8
Fe(1)-C(20)-H(20)	123.0
C(17)-C(18)-C(19)	110(3)
C(17)-C(18)-Fe(1)	69.1(15)
C(19)-C(18)-Fe(1)	71.6(12)
C(17)-C(18)-H(18)	125.2
C(19)-C(18)-H(18)	125.3
Fe(1)-C(18)-H(18)	125.7
C(17)-C(22)-C(20)	106(3)
C(17)-C(22)-Fe(1)	66.6(18)
C(20)-C(22)-Fe(1)	69.1(15)
C(17)-C(22)-H(21)	127.1
C(20)-C(22)-H(21)	127.0
Fe(1)-C(22)-H(21)	128.8
C(18)-C(17)-C(22)	105(2)
C(18)-C(17)-Fe(1)	71.7(16)
C(22)-C(17)-Fe(1)	74.3(18)
C(18)-C(17)-H(17)	127.4
C(22)-C(17)-H(17)	127.4
Fe(1)-C(17)-H(17)	118.8

Table 4. Anisotropic displacement parameters ($\text{Å}^2 \times 10^3$) for m71. The anisotropic displacement factor exponent takes the form: $-2\pi^2[\,h^2a^{*2}U^{11} + ... + 2\,h\,k\,a^*\,b^*\,U^{12}\,]$

	U^{11}	U^{22}	U^{33}	U^{23}	U^{13}	U^{12}
Fe(1)	57(1)	55(1)	52(1)	5(2)	-3(1)	-3(1)
C(2)	80(11)	50(9)	71(14)	-1(10)	-6(8)	-6(7)
C(14)	104(13)	72(11)	41(13)	-36(10)	-7(8)	-3(9)
C(15)	68(9)	75(10)	61(12)	25(10)	-11(8)	-8(8)
C(16)	65(7)	70(9)	58(11)	28(12)	21(8)	8(6)
C(12)	56(7)	54(7)	84(18)	-16(10)	8(7)	7(6)
C(11)	70(9)	60(9)	43(13)	-4(8)	14(6)	8(7)
N(4)	77(7)	49(6)	31(8)	-4(8)	6(6)	-5(4)
N(3)	84(8)	50(7)	25(7)	-6(6)	0(5)	-9(6)
C(9)	43(8)	78(12)	68(13)	20(10)	-6(7)	-14(7)
C(8)	42(6)	60(9)	26(11)	-3(7)	7(5)	7(6)
N(2)	52(6)	45(6)	61(10)	0(7)	4(6)	-4(5)
C(5)	61(9)	31(7)	60(12)	6(8)	-6(7)	3(6)
C(4)	61(8)	72(11)	69(13)	-26(10)	-6(7)	12(7)
C(6)	60(8)	71(10)	45(11)	-13(9)	-4(6)	-11(7)
O(1)	78(7)	137(11)	60(9)	-17(8)	-3(5)	9(7)
C(7)	83(10)	66(10)	52(13)	-14(10)	-2(7)	-3(7)
C(10)	61(9)	57(9)	56(13)	3(9)	15(7)	2(7)
N(1)	115(11)	127(14)	66(12)	-48(11)	-7(9)	-28(10)
O(2)	80(7)	89(8)	61(11)	-19(6)	7(6)	-11(5)
C(13)	78(9)	48(9)	55(12)	16(8)	15(7)	-4(7)
C(3)	63(9)	108(14)	72(14)	-33(13)	-11(7)	2(9)
C(1)	107(14)	112(15)	69(17)	-45(14)	-10(8)	-31(11)
C(19)	230(30)	117(18)	70(20)	11(17)	-30(20)	110(20)
C(20)	138(19)	93(17)	120(30)	67(18)	44(18)	14(14)
C(18)	66(12)	240(40)	200(40)	100(30)	60(20)	81(17)
C(22)	350(50)	90(20)	60(20)	-42(18)	-50(20)	60(30)
C(17)	160(20)	120(20)	300(50)	140(30)	-180(30)	-80(20)

Table 5. Hydrogen coordinates (x 10^4) and isotropic displacement parameters (Å^2x 10^3) for **14**.

	x	y	z	U(eq)
H(14)	5716	-1753	4160	87
H(15)	4793	-1679	6452	82
H(16)	5186	-390	8722	77
H(11)	6345	710	9287	69
H(3N)	7321	1526	9909	63
H(4)	9816	3576	14277	81
H(6)	7761	3980	13590	70
H(7)	7707	4989	16069	80
H(13)	6712	-601	5091	72
H(3)	9738	4480	16856	98
H(1A)	8255	5699	18508	144
H(1B)	8853	4994	19264	144
H(1C)	9045	6008	18240	144
H(19)	6191	-3743	7042	164
H(20)	5503	-3239	9340	142
H(18)	7283	-2791	7149	204
H(21)	6144	-1972	11121	200
H(17)	7209	-1511	9450	234

CHARACTERIZATION OF CATALYST $Fe_3O_4@SiO_2$-1N-EDTA-Eu^{3+}

The X-ray diffraction (XRD) pattern of pure magnetite (Fe_3O_4) and $Fe_3O_4@SiO_2$-1N-EDTA-Eu^{3+} are shown in Figure S15. The relative intensities and characteristic diffraction peaks match well with the standard database peaks of reference pattern (JCPDS file No. 19-0629), verifying the cubic inverse spinel structure of magnetite. Additionally, XRD pattern of $Fe_3O_4@SiO_2$-1N-EDTA-Eu^{3+} reveal broad reflection in the 2θ interval from 20 to 28 ° assigned to the siloxane lattice on the surface of magnetic particles.

Figure S15. X-ray diffraction patterns of Fe_3O_4 and $Fe_3O_4@SiO_2$-1N-EDTA-Eu^{3+}.
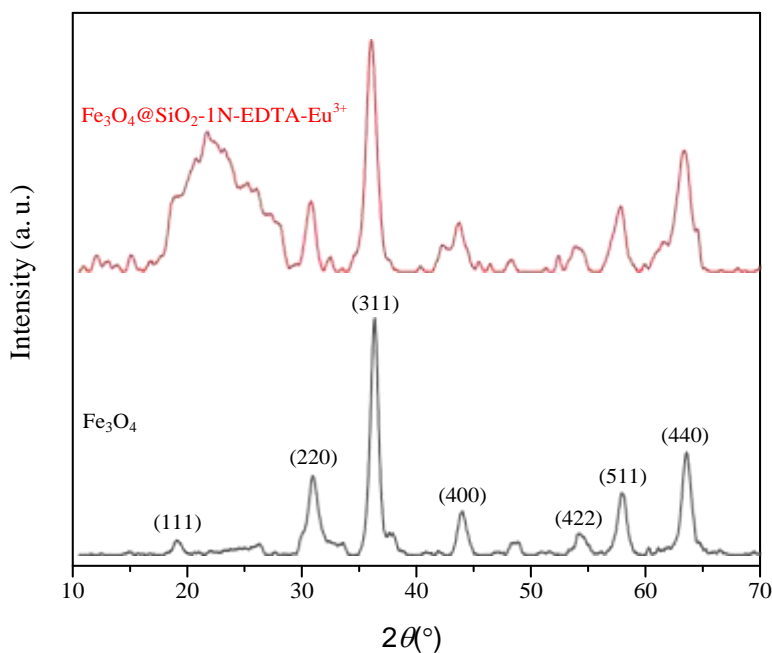
The magnetic properties of Fe_3O_4 and $Fe_3O_4@SiO_2$-1N-EDTA-Eu^{3+} was measured using a vibrating sample magnetometer (VSM) at room temperature under an applied field range of -10000 to 10000 Oe. The field-dependent magnetic measurements (Figure S16) present nearly zero values of coercivity (H_c) and remanent magnetizations (σ_r), revealing that both magnetite and MNP ligand exhibit superparamagnetic behavior.[1-3] The H_c has not varied significantly after functionalization step (7.7 Oe to Fe_3O_4 and 9.0 Oe to $Fe_3O_4@SiO_2$-1N-EDTA-Eu^{3+}), suggesting that no considerable chemical change in the magnetic core.[3] The low value of σ_r to $Fe_3O_4@SiO_2$-1N-EDTA-Eu^{3+}(0.20 emu g^{-1})

indicate that the catalysts cannot retain magnetization before and after exposure to an external magnetic field, which minimizes particle aggregation due magnetic dipole interaction. Furthermore, the difference in the saturation magnetization values (54.5 emu g^{-1} to Fe_3O_4 and 14.3 emu g^{-1} to $Fe_3O_4@SiO_2$-1N-EDTA-Eu^{3+}) may be attributed to the layer of nonmagnetic material on MNP ligand, indicating the effectiveness of particles functionalization.

Figure S16. Variation of the magnetization of of Fe_3O_4 and $Fe_3O_4@SiO_2$-1N-EDTA-Eu^{3+} with the applied field at room temperature.
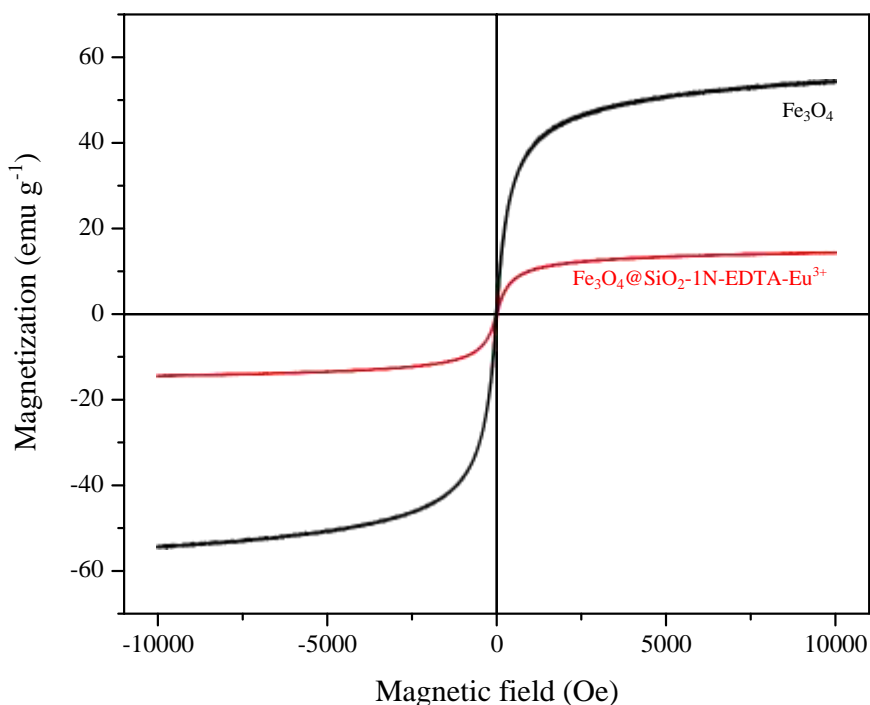
As can be seen in Figure S17, TEM micrograph indicates that Fe_3O_4 particles were successfully functionalized with EDTA. This functionalization process produced a MNP ligand where magnetite nanoparticles are embedded in a siloxane structure. In this regard, the aminoalkylalkoxysilane groups involved in this step may also bind to another alkoxyde group, increasing the extension of the siloxane network.

Figure S17. Representative TEM image of $Fe_3O_4@SiO_2$-1N-EDTA-Eu^{3+}.
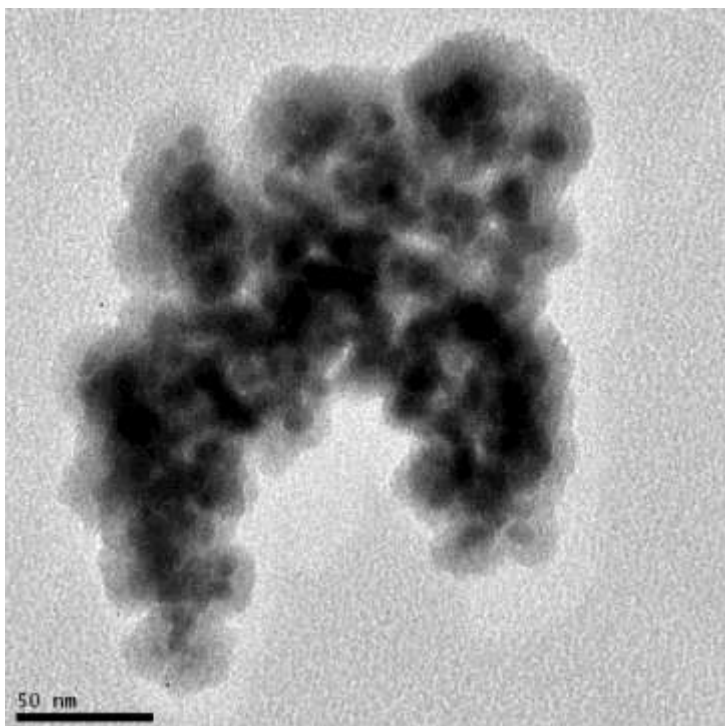
1 X. Pan, J. Guan, J.-W. Yoo, A. J. Epstein, L. J. Lee, R. J. Lee, Cationic lipid-coated magnetic nanoparticles associated with transferrin for gene delivery, *Int. J. Pharm.*, 358 (2008) 263-270.

2 O. Rahman, S. C. Mohapatra, S. Ahmad, Fe_3O_4 inverse spinal super paramagnetic nanoparticles, *Mater. Chem. Phys.*, 132 (2012) 196-202.

3 P. Agrigento, M. J. Beiber, J. T. N. Knijnenburg, A. Baiker, M. Gruttadauria, Highly cross-linked imidazolium salt entrapped magnetic particles - preparation and applications, *J. Mater. Chem.*, 22 (2012) 20728-20735.